Available online at www.sciencedirect.com
SCIENCE DIRECT®
Surface and Coatings Technology 183 (2004) 247–253
SURFACE & COATINGS TECHNOLOGY
www.elsevier.com/locate/surfcoat

Composite plating of Ni–P–Al_2O_3 in two steps and its anti-wear performance

Nabeen K. Shrestha, Dambar B. Hamal, Tetsuo Saji*

Department of Chemistry and Materials Science, Tokyo Institute of Technology, 2-12-1 Ohokayama, Meguro-ku, Tokyo 152-8552, Japan

Received 14 April 2003; accepted in revised form 28 August 2003

Abstract

A composite coating of Ni–P–Al_2O_3 containing 50.0 vol.% of dispersed alumina particles along with approximately 8.9 wt.% (23.4 vol.%) of phosphorus into a nickel matrix was prepared by the proposed 'Two-Step' technique. This technique involves the electrophoretic deposition of a uniform film of alumina particles on a Ni–P-coated copper substrate in the first step followed by the electroless nickel deposition in the second step. The particle incorporated composite coatings exhibited the better anti-wear performance than the particle-free coatings. Heat treatment of these coatings deposited from an electroless bath showed the increased wear resistance of the coating due to the crystallization of hard Ni_3P alloy from the amorphous Ni–P meta-stable phase. However, the referenced electrodeposited coatings exhibited the better anti-wear performance than the electrolessly deposited corresponding coatings in the present investigation.

Keywords: Composite; Electroless; Plating; Nickel; Alumina; Wear

1. Introduction

Ever since the first development of composite materials, the goal has been to achieve a combination of properties not achievable by any of the elemental materials acting alone. A combination of dissimilar materials could produce a composite solid with wide mechanical, chemical, electrical, magnetic and optical properties. However, these properties depend upon the contribution from the distributed and the matrix phases of a composite material. The metal matrix composites containing ceramic particles as a distributed phase find a lot of applications especially in the field of engineering works as anti-wear and anti-frictional materials [1]. There are a number of methods to prepare the particle-dispersed metal matrix composites [2]. However, the most common method is the composite plating. The incorporation of particles into a metal matrix by this method is based on the electro- [3] and electroless [4] plating technique. Since ceramic particles in a particle-dispersed metal matrix composite act as a load-bearing element, a high volume percent of these particles in the composite coating is desirable. Therefore, in an attempt to disperse a high volume percentage of particles in a metal matrix, various cationic surfactants have been used in the plating bath [5,6].

In this regard, recently we have shown that the redox-active cationic surfactant having more positive redox potential than that of the metal being plated acts as a powerful promoter for particle codeposition [7,8]. However, this action of a surfactant depends upon the interaction among particles, surfactant and electrodes. Therefore, a particular surfactant can be used for enhancing the codeposition of only a limited type of particles. In order to overcome this difficulty, recently we have reported a simple technique for incorporating a high volume percent of various ceramic particles into nickel matrix in two steps [9], and we have demonstrated that these composite coatings had a better anti-wear performance than the composite coatings prepared by the classical technique of single-step composite plating. However, a close control of pH of the bath is needed in this method and it is tedious to find out the electrolysis potential of the second step. Moreover, it took several hours of electrolysis time to prepare these composites. Therefore, in an attempt to overcome these problems, electro-

*Corresponding author. Tel./fax: +81-3-5734-2627.
E-mail address: tsaji@o.cc.titech.ac.jp (T. Saji).

0257-8972/04/$ - see front matter © 2003 Elsevier B.V. All rights reserved.
doi:10.1016/j.surfcoat.2003.08.085

Table 1
Bath composition and operating conditions

$NiSO_4 \cdot 6H_2O$	30 g dm^{-3}
$NaH_2PO_2 \cdot H_2O$	40 g dm^{-3}
Lactic acid (85–92%)	40 cm^3 dm^{-3}
Succinic acid	5 g dm^{-3}
Sodium fluoride	2 g dm^{-3}
pH	6.0
Temperature	65 °C
Volume/area	10
Plating time	90 min

less plating of nickel was carried out in the second step of the present study. It is well known that the electroless plating produces a fine and smooth coating compared to the coating produced by an electrodeposition technique. Moreover, the mechanical [10,11] and chemical strength [12,13] of a nickel coating can be increased by incorporating elemental phosphorus from an electroless plating bath containing sodium hypophosphite as a reducing agent.

2. Experimental

2.1. First step (*electrophoretic deposition*)

As a substrate, a copper plate with the dimension of $20 \times 50 \times 0.3$ mm^3 was polished with the metal polishing reagent (Pikal, Nihon Maryo-kogyo Co., Ltd) to mirror finish followed by ultrasonic cleaning with acetone and chloroform for 5 min. The surface of this copper plate was first activated with palladium and a thin film of Ni–P was coated onto this copper plate for 5 min using the electroless plating bath shown in Table 1. This substrate was placed vertically at a distance of 1 cm parallel to a graphite anode plate and electrophoretic deposition [9] of alumina particles (α-type, average particle size 0.5 μm, Wako Pure Chemical Industries, Ltd, Japan) on this substrate was carried out using an ethanol bath containing 2 mM $MgCl_2 \cdot 6H_2O$ and a suspension of 16 g dm^{-3} of the particles. These particles were suspended by agitating the bath ultrasonically for 10 min using an ultrasonic disruptor (Tomi Seiko, UP-200P) followed by stirring the bath for 10 min just before the deposition. Electrophoretic deposition was performed under an electric field strength of 50 V cm^{-1} for 1 min.

2.2. Second step (*deposition of nickel*)

The substrate covered with the electrophoretic deposits was subjected to the electroless plating of nickel for 90 min in an acidic hypophosphite bath shown in Table 1. The composite coating thus produced was sonicated in acetone to remove the particles that were loosely bounded to the surface. In order to compare the anti-wear performance of the electroless and electrodeposited coatings, a $Ni–Al_2O_3$ composite coating was prepared by the electrodeposition of nickel in the second step as follows. A copper substrate coated with electrophoretic deposit of alumina was subjected to the electrodeposition of nickel using a nickel chloride bath (pH 6.7) containing 50 g dm^{-3} $NiCl_2 \cdot 6H_2O$ and 10 g dm^{-3} NH_4Cl. A controlled potential electrolysis was carried out at a constant potential of −0.80 V vs. SCE for the time taken to pass 40 C cm^{-2} of charge at 25 °C [9]. Similarly, particle-free electroless and electrodeposition of nickel was carried out on the copper substrates under similar conditions from the same kind of respective baths as described above.

2.3. Analysis of deposits

A scanning electron microscope (SEM) was used to study the surface and cross-sectional morphology of the coatings. Thickness of the deposits was measured directly from the SEM micrograph of the cross-section of a coating. This section of the coating was prepared as follows. A thin layer of nickel was electrodeposited on one side of a carbon plate ($10 \times 30 \times 1$ mm^3, NILACO, Japan) while the other side of the plate was blocked with a PVC adhesive tape. This nickel-coated carbon plate was used as a substrate for the composite coating by the electrodeposition of nickel in the second step, while a thin film of Ni–P was coated to this nickel-coated carbon plate to use it as a substrate for the composite coating by the electroless deposition of nickel in the second step. These two substrates were then subjected to the composite plating of $Ni–Al_2O_3$ and $Ni–P–Al_2O_3$ as described earlier by the proposed two-step method. After ultrasonic cleaning of these coatings on the carbon plate, approximately 3 mm from the top of the plate on the other side was scratched with a paper knife to an approximate depth of the half of a thickness of the carbon plate. Then, this plate was broken through the scratched line and the cross-section of the composite coating was examined using a SEM. The percentage of phosphorus, nickel and alumina in the composite coatings was determined using an energy dispersed X-ray micro-analyzer (EDX) coupled to the SEM.

Ni–P and $Ni–P–Al_2O_3$ composite coatings were treated thermally at 400 °C for 60 min. The effect of the heat treatment on the crystal structure of these deposits was studied using an X-ray powder diffractometer.

Anti-wear performance of the composite coatings was evaluated using an abrasion tester (NUS-IS03, SUGA Test Instruments Co. Ltd, Japan). A wheel of 50 mm diameter mounted with a SiC abrasive paper (~10-μm-grit size, 1500 CC-CW, SANKO, Japan) was used as the counter surface. This counter wheel was pressed against the specimen under various loads (5–24.5 N) and the specimen was moved to-and-fro against the

counter surface under dry sliding conditions at a constant speed of 40 cycles min^{-1} for 300 cycles at room temperature in air. For each back-and-forth movement of the specimen, the counter wheel rotated by a specific fraction proving a fresh abrasive paper for the next cycles. Thus, this back-and-forth movement of the specimen gave a worn dimension of 33 mm long and 10 mm wide. Before and after the wear test, the samples were sonicated for 5 min in acetone and dried in warm air and then, weighed. The comparative degree of wear resistance of various coatings was assessed under different applied loads and has been expressed here in terms of the reciprocal of weight loss in milligram per 300 cycles.

3. Results and discussion

In the electrophoretic experiment, magnesium salt was used in order to charge the particles. Adsorption of Mg^{2+} ions on the particles gives a positive charge to the particles and hence, these charged particles move to the cathode under an electric field. On approaching the cathode, the electrical field exerts sufficient force to overcome the mutual repulsion between particles, thus allowing them to come close enough for the London–van der Waals forces of attraction to predominate. Thus, particles are deposited on the cathode and the adhesion of these deposits is due to the London–van der Waals forces of attraction [14]. On the other hand, Mg^{2+} ions react with water and alcohol to give the corresponding hydroxide and alkoxide. It is possible that the presence of these oxides between the particles may enhance the effect of the van der Waals forces and result in an adherent deposit [14,15]. The adhesion strength of the electrophoretic deposits was also found to depend on the morphology of the coating. When these deposits were uniform, their adhesion strength was stronger. However, without ultrasonic agitation of the bath, the electrophoretic deposits consisted of agglomerated particles. When the substrate coated with such agglomerated deposits was immersed into the electroless nickel bath in the second step, these deposits soon dislodged from the electrode and dropped down to the electrolyte. On the other hand, the stability of the particle suspension in an ultrasonically agitated bath was longer. Therefore, the electrophoretic deposition in the present study was performed without stirring the bath during the deposition. SEM micrographs revealed that the electrophoretic deposits prepared in the first step of composite coating had a uniform distribution of alumina particles and the coating had a uniform thickness of approximately 38 μm. As described in our previous paper [9], such deposits contain a network of pores through which the electrolyte from the plating bath diffuses into the substrate and reduction of nickel ion takes place. This deposited nickel grows through the opening of the porous network and binds the alumina particles in the second step.

In order to deposit nickel and elemental phosphorus in the second step, an electroless bath with hypophosphate as a reducing agent in acidic media was used. Composition and operating conditions of this bath for the electroless deposition of nickel in the second step are given in Table 1. In this bath, lactic acid was used as a complexing agent, while succinic acid and sodium fluoride were used as exaltants in order to enhance the oxidation of hypophosphite ion. Beside this bath, other types of electroless bath were also studied for the nickel deposition in the second step of this composite plating. The rate of nickel deposition from an alkaline-citrate bath [4] was very slow, whereas the rate of evolution of hydrogen gas associated with the reduction of nickel ions was vigorous in an alkaline-pyrophosphate bath, which destroyed the electrophoretic deposits.

No reduction of nickel ion from the above bath was observed even at the surface of a bare copper plate without activation of the surface with palladium. On the other hand, there was no definite time for the initiation of nickel deposition at the surface of Pd-activated copper substrate covered with an electrophoretic deposit. When this substrate was dried in a warm air or was left for a prolonged time (5–6 days), reduction of nickel ion from this bath (Table 1) was hardly possible on the surface of such a substrate. This is probably due to the formation of an oxide of copper, which deactivates the surface [16]. Therefore, the Pd-activated copper substrate was modified into Ni–P by depositing a thin film of Ni–P, and then, the substrate was subjected to the electrophoretic deposition. In this case, reduction of nickel ion on the surface of such substrate covered with the electrophoretic deposits started within 3 min of immersion of the substrate into the bath. On the other hand, a prolonged leaving period of such substrate had no adverse effect on the reaction initiation of nickel deposition in the second step.

A pH range of 5.0–6.0 and a temperature of 65 °C was selected for depositing nickel in the second step for 90 min. After using this bath for 90 min, the pH of the bath hardly changed by 0.5 units. This optimized bath was used without stirring, since even the slow stirring swept the electrophoretic deposits away from the substrate. Temperature and pH of the bath had a great influence in producing a uniform composite coating in the second step. When the bath temperature and pH were increased higher than 70 and 6.0 °C, respectively, deposition of nickel was associated with the brisk evolution of hydrogen gas, which immediately destroyed the alumina deposits. On the other hand, the bath was inactive at a temperature lower than 50 °C, whereas the deposition of nickel did not proceed for a long time at a pH lower than 4.5. As a result, the so-far-deposited nickel could not bind the alumina deposits tightly in the

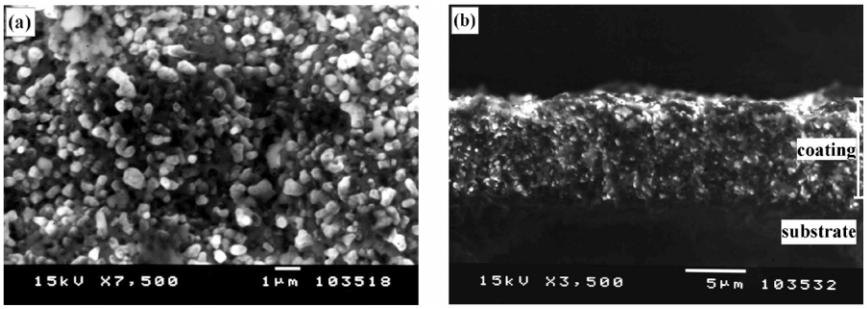

Fig. 1. SEM micrographs of (a) surface and (b) cross-section of the Ni–P–Al_2O_3 composite coating prepared by the electroless deposition of nickel in the second step using the bath shown in Table 1.

matrix so that the deposits could be removed easily from the substrate even with a finger.

Surface and cross-sectional morphologies of the Ni–P–Al_2O_3 composite coating prepared by the proposed two-step method are shown in Fig. 1a and b. These SEM micrographs show the uniform distribution of Al_2O_3 particles through out the deposits and it has a uniform thickness of approximately 9 μm for 90 min of electroless deposition at 65 °C. Similarly, SEM micrographs in Fig. 2a and b are the image of surface and cross-section of the electrodeposited Ni–Al_2O_3 coating, respectively, which indicate the uniform particles' distribution and a uniform thickness of approximately 17 μm for approximately 15 h of electrodeposition. These SEM micrographs confirm the uniform distribution of Al_2O_3 particles throughout the composite coatings prepared in two steps.

From the EDX measurements, the Ni–P coating was found to contain 12.1 wt.% phosphorus and the Ni–P–Al_2O_3 coating constituted with 8.9 wt.% of phosphorus and 41.7 wt.% (50.0 vol.%) of alumina. Similarly, the electrodeposited Ni–Al_2O_3 coating was found to contain approximately 67.0 vol.% of alumina. With the variation of pH (4.5–6.0), concentrations of nickel sulfate (25–30 g dm^{-3}) and sodium hypophosphite (25–45 g dm^{-3}), no significant change in phosphorous content of the coatings was obtained.

Fig. 3a is the XRD pattern of a Cu-substrate used in the present investigation and XRD patterns of the Ni–P coating before and after heat treatment are shown in Fig. 3b and c, respectively. Similarly, XRD patterns of the as-deposited and the heat-treated Ni–P–Al_2O_3 composites are shown in Fig. 4a and b, respectively. The most intense peak at 50.55° in Fig. 3a,b and Fig. 4a is due to Cu (2 0 0) plane of the Cu-substrate. Comparing the XRD patterns in Fig. 3a and b, there are no new additional well-defined peaks in Fig. 3b indicating the deposits of the as-deposited Ni–P coating consisted of an amorphous nickel. After the heat treatment of this Ni–P coating, new additional peaks in its XRD pattern (Fig. 3c) at 30.28, 36.52, 41.83, 41.97, 42.88, 43.56, 43.77, 44.64, 46.76, 51.93, 52.90, 55.56, 58.97, 75.53 and 78.85° were observed. The most intense peak is due to the precipitation of Ni (1 1 1), whereas all the other additional new peaks appeared after the heat treatment of the Ni–P coating are due to the change of the amorphous nickel and phosphorous into the crystalline N_3P alloy. A similar phenomenon of crystallization of a meta-stable Ni–P into a stable Ni_3P alloy has been reported previously in Refs. [1,17,18]. The X-ray dif-

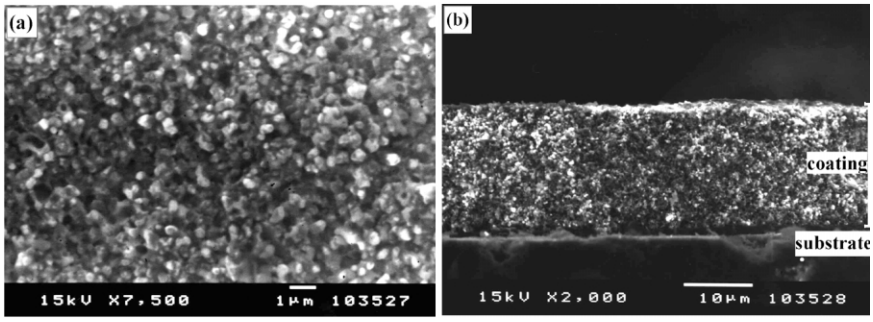

Fig. 2. SEM micrographs of (a) surface and (b) cross-section of the Ni–Al_2O_3 composite coating prepared by the electrodeposition of nickel in the second step using a bath containing 50 g dm^{-3} $NiCl{\cdot}6H_2O$, 10 g dm^{-3} NH_4Cl, pH 6.7, electrolysis at −0.80 V vs. SCE for 40 C cm^{-2}, 25 °C.

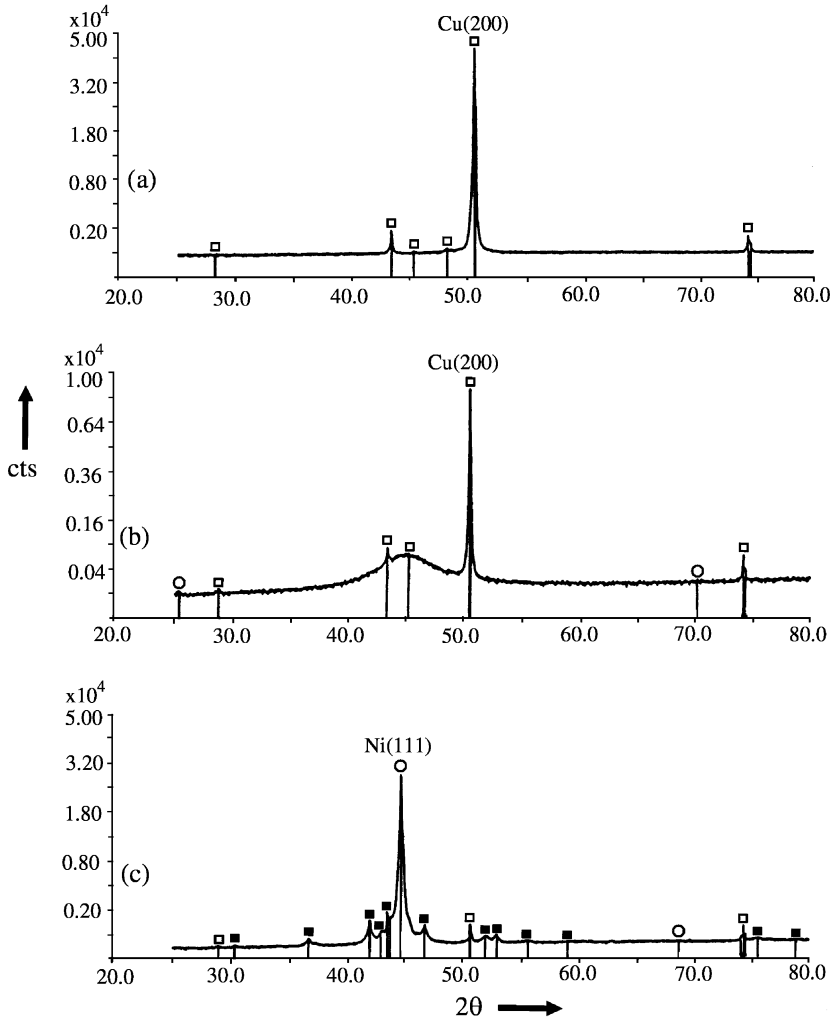

Fig. 3. XRD pattern of the (a) copper substrate, (b) as-deposited Ni–P coating prepared using the bath shown in Table 1, and (c) heat-treated Ni–P coating at 400 °C for 1 h. Cu (□); Ni (○); Ni_3P (■).

fraction peaks at 35.40, 37.04, 52.82, 57.67, 66.67 and 76.70° in Fig. 4 indicate the presence of α-type alumina in the particle incorporated Ni–P–Al_2O_3 coating. Like the case of the heat-treated Ni–P coating (Fig. 3c), new peaks after the heat treatment of this Ni–P–Al_2O_3 coating (Fig. 4b) have appeared. As explained earlier, these additional peaks at 36.38, 41.80, 42.91, 43.44, 45.25, 46.62, 50.54, 51.81, 52.6, 55.31, 57.54 and 75.31° in Fig. 4b are also due to the crystallization of a meta-stable Ni–P amorphous phase into a stable Ni_3P alloy, whereas the most intense peak at approximately 44.5° is due to the precipitation of the Ni (1 1 1).

Fig. 5 shows the variation of weight loss with various applied loads for the particle-free and the particle incorporated coatings. In all cases, the wear of the coatings has increased with the applied loads. This is probably due to an easy penetration of the SiC abrasives into the coatings at higher applied loads, resulting in excessive material removal from the worn surface of the coatings. However, the material removal has reduced markedly in the case of particle incorporated coating due to the resistance of the micro-cutting action of abrasives by the reinforcement of hard and anti-wear alumina particles. On the other hand, the heat-treated particle-free and particle incorporated coatings have exhibited the better anti-wear performance compared to the corresponding as-deposited coatings. This improved wear resistance of the heat-treated coatings is probably due to the crystallization of the meta-stable Ni–P amorphous phase into most stable Ni_3–P phase, which increases the hardness of the composite matrix [1,19–22]. In the present investigation, the as-deposited Ni–Al_2O_3 coating exhibited the best anti-wear performance among all the other coatings. This better anti-wear performance is probably due to its higher volume percentage of incorporated alumina particles [9] and due to the contribution from the nickel matrix as well. As evident in Fig. 5, the wear resistance of the as-deposited electrodeposited Ni-

coating is higher than that of the as-deposited electroless Ni–P coating and is closer to the wear resistance of the heat-treated Ni–P coating. On the other hand, the wear resistance of the as-deposited Ni–Al_2O_3 is higher than that of the as-deposited Ni–P–Al_2O_3 coating and is closer to the wear resistance of the heat-treated Ni–P–Al_2O_3 coating. In the present investigation, the above results revealed that the wear resistance of the electrodeposited Ni-coating is higher than that of the electrolessly deposited amorphous coating of Ni–P deposits and its wear resistance is closer to that of the Ni_3P alloy. Therefore, the better anti-wear performance of the Ni–Al_2O_3 coating than that of the Ni–P–Al_2O_3 coating might be mostly due to the contribution from the electrodeposited Ni-matrix. The magnitude of the anti-wear performance of the Ni–Al_2O_3 is not very much different from that of the heat-treated Ni–P–Al_2O_3 coating. However, the second step for the Ni–Al_2O_3 coating takes approximately 4 h at 25 °C in order to produce a deposit of 9-μm thick [9], while the present technique produces the same thick deposits in 90 min.

Wear tracks of all the composite coatings were also examined using a SEM. The wear tracks of the as-deposited particle-free Ni–P and particle incorporated Ni–P–Al_2O_3 coatings at the end of 300 cycles under the load of 24.5 N are shown in Fig. 6a and b, respectively. A similar wear track was also observed in the case of corresponding heat-treated coatings. In the case of particle-free coatings, the surface became smoother and shining after the wear test, though the material lost in this case was relatively higher. This development of shining surface is due to the polishing action of the abrasive action of the hard SiC counter surface. However, the presence of alumina particles was found to resist the coating to a greater degree from being surface damaged and material lost. The SEM

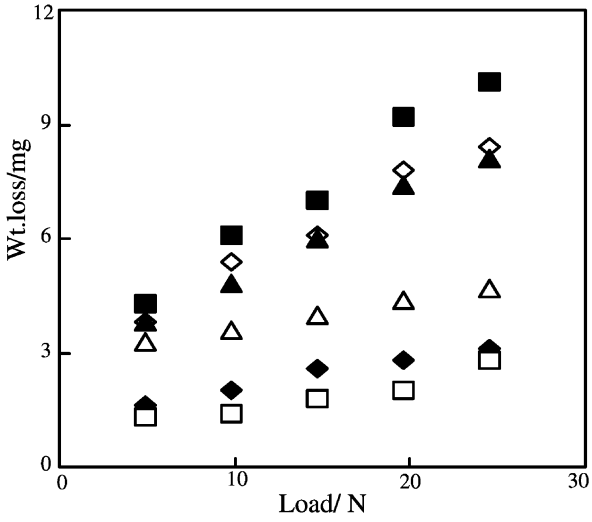

Fig. 5. Wear of the composite coatings at various applied loads. As-deposited Ni–P coating (■); heat-treated Ni–P coating (◇); without heat treated electrodeposited Ni-coating (▲); as-deposited Ni–P–Al_2O_3 coating (△); heat-treat Ni–P–Al_2O_3 coating (♦); as-deposited Ni–Al_2O_3 coating (□) prepared by the electrodeposition of nickel in the second step using a bath as described in Fig. 2.

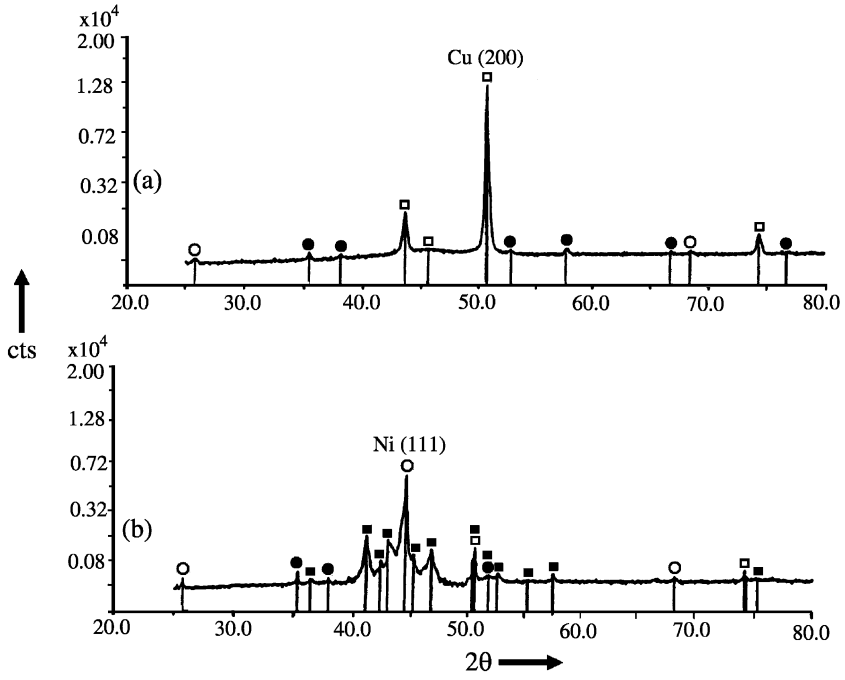

Fig. 4. XRD pattern of the Ni–P–Al_2O_3 composite coating prepared as described in Fig. 1. (a) As-deposited, and (b) after heat treatment at 400 °C for 1 h. Cu (□); Ni (○); α-Al_2O_3 (●); Ni_3P (■).

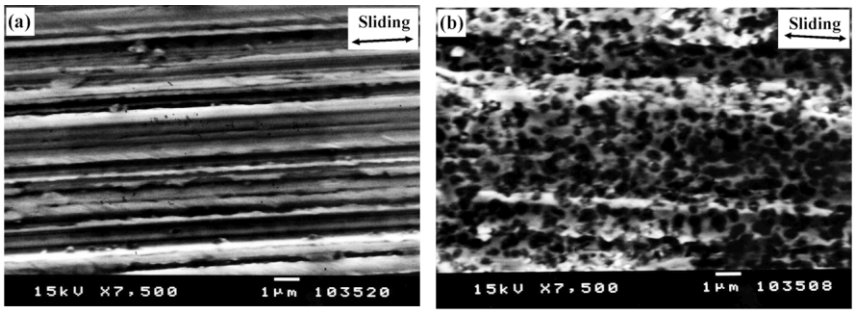

Fig. 6. Wear tracks of the heat-treated (a) Ni–P and (b) Ni–P–Al_2O_3 coatings at the end of 300 cycles under the load of 24.5 N.

micrograph of the wear track for this particle incorporated coating (Fig. 6b) shows only the abrasive groves whose size is about the same as that of the incorporated particles (Fig. 1a). These wear tracks indicate that the wearing of the coating consisted of the ploughing the particles out of the matrix by the counter surface.

4. Conclusions

The present investigation shows that high volume percentage of alumina particles can be uniformly dispersed into a nickel matrix using the proposed two-step composite coating method. The deposition of nickel in the second step in a substrate covered with an electrophoretic deposits can be carried out faster without destroying the electrophoretic deposits by the electroless plating technique compared to that by the electrodeposition method.

The X-ray diffraction studies of the coating prepared from an electroless plating bath revealed that a solid phase inter-diffusion of nickel and phosphorus takes place after the thermal treatment of the coating. As a result, there is crystallization of a hard Ni_3P alloy. Probably, this is the reason for better anti-wear performance of the heat-treated Ni–P and Ni–P–Al_2O_3 coatings than the same coatings without the thermal treatment. However, the particle-free electro-deposited Ni-coatings exhibited the better anti-wear performance than the corresponding electrolessly as-deposited Ni–P coating due to the amorphous phase of the nickel because of the higher amounts of phosphorous content. Therefore, it is needless to say that further work is required in order to coat the substrate with the composite coating containing different amounts of phosphorous, especially in the lower content range for the further enhancement of the anti-wear performance of the Ni–P–Al_2O_3 composite coating.

Acknowledgments

This research was supported by a Grant-in-Aid for Scientific Research (No. 14550699) from the Ministry of Education, Science and Culture, Japan. The authors would like to thank Mr S. Genseki and Mr J. Saeki for the EDX and XRD data, respectively.

References

[1] G. Straffelini, D. Colombo, A. Molinari, Wear 236 (1999) 179.
[2] I. RajGopal, Bull. Electrochem. 8 (1992) 384.
[3] J.K. Dennis, T.E. Such, Nickel and Chromium Plating, second ed., Butterworth and Co. Ltd, 1986.
[4] G.O. Mallory, J.B. Hajdu, Electroless Plating, American Electroplaters and Surface Finishers Society, 1990.
[5] R.F. Ehrsam, US Patent, 4043878.
[6] A. Hovestad, L.J.J. Janssen, J. Appl. Electrochem. 25 (1995) 519.
[7] N.K. Shrestha, I. Miwa, T. Saji, J. Electrochem. 142 (2001) C106.
[8] N.K. Shrestha, M. Masuko, T. Saji, Wear 254 (2003) 555.
[9] N.K. Shrestha, S. Sakurada, M. Masuko, T. Saji, Surf. Coat. Technol. 140 (2001) 175.
[10] J.S. Chen, J.G. Duh, Surf. Coat. Technol. 139 (2001) 6.
[11] W. Yucheng, L. Guanghai, Z. Lide, Y. Bo, Z. Metallkd. 91 (2000) 788.
[12] W. Sha, C.J. Murphy, J. Quinn, J. Alloys Compd. 287 (1999) 27.
[13] P.H. Lo, W.T. Tsai, J.T. Lee, M.P. Hung, Surf. Coat. Technol. 67 (1994) 27.
[14] D.R. Brown, F.W. Salt, J. Appl. Chem. 15 (1965) 40.
[15] B.E. Russ, J.B. Talbot, J. Electrochem. Soc. 145 (1998) 1253.
[16] I.V. Petukhov, E.V. Kuznetsova, Prot. Metals 27 (1991) 261.
[17] K.H. Hur, J.H. Jeong, Dong, N. Lee, J. Mater. Sci. 25 (1990) 2573.
[18] J.C. Doong, J.G. Duh, Surf. Coat. Technol. 58 (1993) 19.
[19] O.A. Leon, M.H. Staia, H.E. Hintermann, Surf. Coat. Technol. 120–121 (1999) 641.
[20] D.H. Cheng, W.Y. Xu, L.Q. Hua, Z.Y. Zhang, X.J. Wan, Plat. Surf. Finish. 85 (1998) 61.
[21] R.J. Keyse, C. Hammond, Mater. Sci. Technol. 3 (1987) 963.
[22] D.T. Gawne, U. Ma, Mater. Sci. Technol. 3 (1987) 228.